

From Dominoes to Bridges: Application of Domino Wave Propagation Mechanisms in Cascading Collapse Prevention

Zhiting Yu

Shanghai Qibaodwight high school, Shanghai, 201101, China

Abstract. Focusing on the domino effect in physics, this study discusses the influence of factors such as domino spacing, mass, shape, and friction on wave velocity and propagation stability through the analysis of angular momentum conservation, energy attenuation coefficient, and collision torque. In engineering applications, the study applies domino wave propagation to the phenomenon of chain collapse in bridge engineering. The study analyzes the triggering role of external factors such as floods, scour, collisions, overloads, earthquakes, and fires in bridge structural failure, pointing out that the bridge collapse process conforms to the domino model of "local instability-chain reaction-overall collapse." The study suggests that in bridge design and maintenance, structural redundancy or damping devices can be installed at the seventh and eighth "critical nodes" to effectively block the transmission path of the "collapse wave," thereby preventing or mitigating the risk of chain collapse of bridges. This paper provides new ideas for the translation of the domino model into engineering practice and is of great significance.

Keywords: Domino effect; wave propagation; cascading collapse; bridge failure.

1. Introduction

The domino effect is a very common phenomenon in the world. According to the principles of physics, the domino effect involves force, energy transfer, and momentum. Dominos need a push to start their movement, which can be friction, the friction that arises from the push. As the dominoes fall, their gravitational potential energy is converted into kinetic energy, and momentum is transferred between the dominoes. These physical interactions sustain the chain reaction. This transfer of potential energy during the fall allows long chains of dominoes to form spectacular displays, popular worldwide.

The domino effect has been extensively studied by modern scholars. Efthimiou first proposed and defined the domino wave model, simplifying it to a rod system with a terminal velocity (Koellhoffer, 2005). Studies have examined both single domino models and domino chains, finding that the falling speed varies with the number of dominoes in the chain. (Polaner Shafer) based his discovery on his idealized model of domino blocks and how he used conservation of energy, and then shifted his attention from individual blocks to arrays of more optimistic models of dominoes. (FUJII) After the actual experiment and computer program simulation, Fujii, based on the colliding wave between domino blocks, finally identified the regularity of increasing velocity. He developed a simple rod model into a two-dimensional mathematical theoretical model for dominoes and proposed a theory that, under the same spacing between domino blocks in a falling array, the velocity reaches its peak when the 6th to 7th block falls.

Beyond this theory, (Daniel Ding et al. 2022) developed a more mature theory by connecting rigidity to Efthimiou's assumption. In their model, the speed of domino waves does not exceed the wave speed in the domino chain with elastic contact.(Shi et al.) estimated the interaction between dominoes and the ground, taking friction and the influence of different weights into account. By introducing additional conditions, they incorporated more variables beyond the ideal rod model and identified the conditions for the emergence of solitary waves. Their research also analyzed variations in spacing and size among groups, calculated relevant data, and explained that solitary waves were observed because the small contribution to mechanical energy in the system did not significantly affect subsequent blocks. (Lu et al.) discovered the effect of specific shapes and blockings on domino wave propagation. The shapes of the chosen blocks ranged from spheroid to cube. In general, the

wave velocity in the dynamic system of domino blocks is mainly affected by their spacing, mass, shape, and position in the array. Following this research, the theory of the domino effect and its wave phenomenon has been clarified. Based on the review of the above papers, in reality, problems such as bridge failure and collapse caused by the domino effect can be effectively prevented through a deeper understanding of the characteristics of domino wave transmission. Their research still involves several potential future topics, such as the scale at which tangential forces significantly affect wave propagation speed. Gravity performs non-zero work and exerts non-zero torque. Multiple interactions are possible between consecutive dominoes. The structure of this paper will later discuss the period of domino waves and consider the effects of the aforementioned materials on the spacing, size, mass, and shape of the blocks. To avoid the hazards of domino waves in real-world scenarios, the ideal improvement is to set an obstruction in front of the 7th and 8th blocks to stop or delay their fall, since the wave's acceleration becomes constant after this series. This relates to the later discussion topic—how to control and prevent wave phenomena in bridges.

2. Methodology

2.1 Single Block Analysis

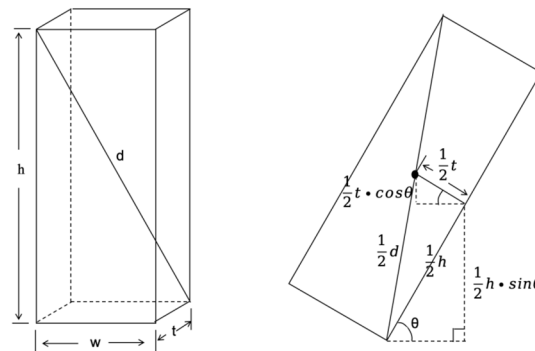


Figure 1: Geometric parameters of the Single Block

Symbols: Height of the domino (h), Width of the domino (w), Thickness of the domino (t), Diagonal of the domino (d), The tilt angle of the domino relative to the horizontal (θ).

In Steve Koellhoffer's essay *Falling Domino*, a mathematical model is presented in which each domino block is treated in physics as an ideal rigid body of uniform density. The center of mass is located at the intersection of the two diagonals, i.e., at the geometric center. The block is assumed to pivot about a fixed, frictionless axis through one of its lower edges; all dissipative forces are neglected. The subsequent motion is then governed by the conservation of mechanical energy and the conservation of angular momentum.

$$E_p = mg \left(\frac{t}{2} \cos\theta + \frac{h}{2} \sin\theta \right) \quad (1)$$

$$E_k = \frac{1}{2}mv^2 + \frac{1}{2}I\omega^2 \quad (2)$$

$$I = \frac{1}{3}m\Delta h^2 \quad (3)$$

$$v = r\omega = \frac{d}{2}\omega \quad (4)$$

By substituting v , we can get the Kinetic energy expression formula

$$E_{kinetic} = \frac{1}{24}m\omega^2(3d^2 + 4\Delta h^2) \quad (5)$$

So, the total energy comes with:

$$E_{total} = mg \left(\frac{t}{2} \cos\theta + \frac{h}{2} \sin\theta \right) + \frac{1}{24}m\omega^2(3d^2 + 4\Delta h^2) \quad (6)$$

When the domino block begins to fall,

$$E_{pi} = \frac{1}{2}mgh = mg \left(\frac{t}{2} \cos\theta_i + \frac{h}{2} \sin\theta_i \right) \quad (7)$$

That time, the initial potential energy is equal to the total energy.

$$E_{pi} = E_{tt} \quad (8)$$

$$mg \left(\frac{t}{2} \cos\theta_i + \frac{h}{2} \sin\theta_i \right) = mg \left(\frac{t}{2} \cos\theta + \frac{h}{2} \sin\theta \right) + \frac{1}{24} m\omega^2 (3d^2 + 4\Delta h^2) \quad (9)$$

After simplification and merging terms, we can get:

$$\omega = \sqrt{\frac{12tg(\cos\theta_i - \cos\theta) + 12tg(\sin\theta_i - \sin\theta)}{3d^2 + 4\Delta h^2}} \quad (10)$$

The θ_i is known as the initial angle, θ is equal to zero because it falls to the horizontal.

$$\omega = \sqrt{\frac{12tg(\cos\theta_i - \cos\theta) + 12tg(\sin\theta_i - \sin\theta)}{3d^2 + 4\Delta h^2}} \quad (11)$$

$$\omega_{final} = \sqrt{\frac{12tg(\cos\theta_i - 1) + 12tg(\sin\theta_i)}{3d^2 + 4\Delta h^2}} \quad (12)$$

Where ω_{final} shows the centre of mass of a domino and its effect on the velocity speed.

2.2 Multi-Block Analysis

Efthimiou and Fujii's theories evaluate the blocks' interaction with the same center of mass, size, material, and spacing of ideal collision unit. So, by combining the two theories above, imagine the rods are blocks, which means that they have thickness, to create a more complex and well-considered model to determine two blocks collision.

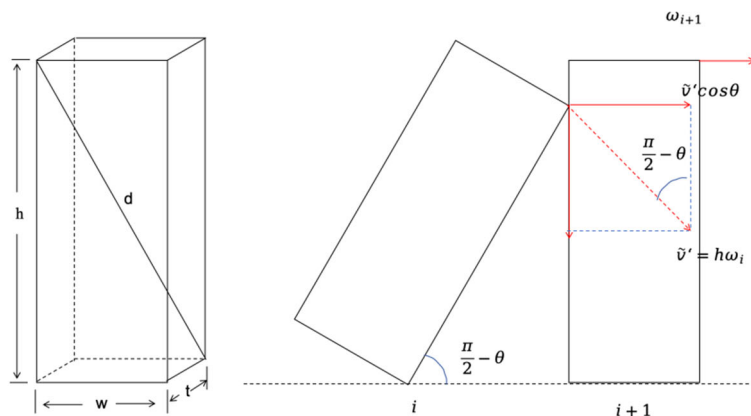


Figure 2: Geometric parameters of Multi Block (Mixed from theories from (FUJII) and (Efthimiou and Johnson) and revised here)

The system of equations can be solved easily for ω_{k+1} and ω_k :

$$\omega_{k+1} = f + \omega_{nk} \quad (13)$$

$$\omega_{nk} = \frac{\omega_{k+1}}{f} \quad (14)$$

Where $f_{\pm} = \frac{2}{\cos^2\theta \pm \frac{1}{\cos^2\theta}}$

Consider the kth rod as it falls from the vertical at an angle θ , its position just before the collision. Conservation of total energy yields

$$\frac{1}{2}I\omega_k^2 + mgl = \frac{1}{2}I\omega_{nk}^2 + mgl \cdot \cos\theta \quad (15)$$

or

$$\omega_{nk}^2 = \omega_k^2 + \frac{2g}{l}(1 - \cos\theta) \tag{16}$$

By combining formulas

$$\omega_{k+1}^2 = f^2 + \omega_k^2 + b \tag{17}$$

Where $b = \frac{2g}{l}f^2(1 - \cos\theta)$

While that ω_1 is the initial angular velocity of the first rod caused by the initial external push. We show now that $f < 1$. Since $\theta \neq 1,0$. Then $(\frac{x-1}{x})^2 > 0, \frac{x^2+1}{x^2} > 2$. From the last inequality it follows that $f = \frac{2}{(\frac{x^2+1}{x^2})} < 1$

Since $f < 1$ it follows that $\lim_{n \rightarrow +\infty} f^n = 0$

$$\lim_{n \rightarrow +\infty} \omega_k^2 = \frac{2g}{l}(1 - \cos\theta) \frac{f_+^2}{1 - f_+^2} = \omega^2 \tag{18}$$

Thus, deep in the chain we find translational invariance: the initial angular velocity imparted to a rod by its neighbors is independent of its position. Note that in this limit the initial thrust applied to the first rod becomes irrelevant.

Based on the mathematical model used in the derivation in Section 2.1, now place two identical domino blocks at a certain distance from each other, allow the first one to fall freely, rotate around the pivot, and then collide and push the next one to achieve the maximum velocity.

2.3 Two blocks of domino model the relationship of torques

Unlike the previous situations, which were fixed, both the collision position and the block are free to move.

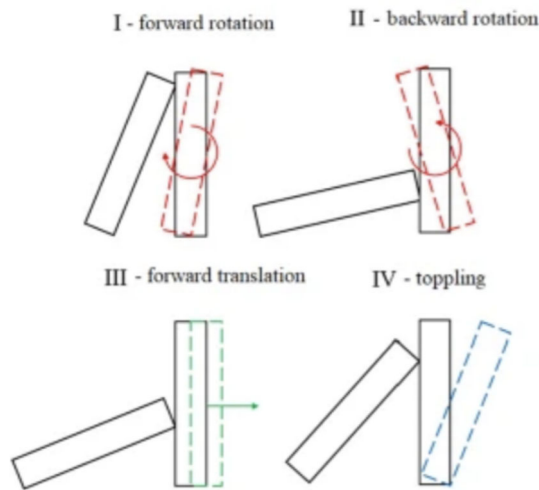


Figure 3: Torque of multi-block

It is convenient to give the bound in terms of the magnitude of the contact force emerging during a harmonic collision.

$$\int_0^{T_e} F_x dt = \cos \beta \int_0^{T_e} F_m \sin\left(\frac{\pi}{T_c} t\right) dt = m'v = m'\omega l \cos \beta \tag{19}$$

This leads to

$$F_m = \frac{\pi m \omega l}{2 T_c \cos^2 \beta} \tag{20}$$

2.4 Transmission of energy in an array of domino blocks

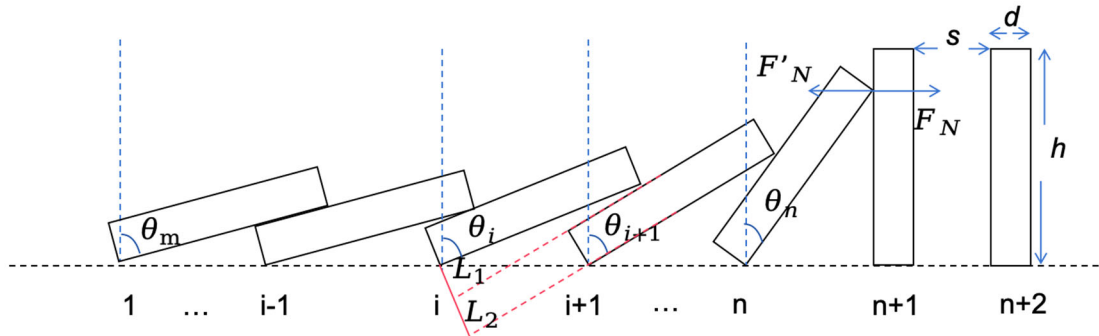


Figure 4: Geometric parameters of domino array (Quoted from Toppling dynamics of mass-varying dominoes [Shi,2019], REPRODUCED)

$$k = 1 - \frac{\sqrt{s^2 + 2sd}}{h} \tag{21}$$

Where k is the attenuation exponent of the domino’s motion.

This effectively describes the domino velocity during the collapsing, including both the initial falling velocity and the velocity during the fall. Explaining the relationships between the motion and the distance between blocks, and the length and thickness of the block. On the other hand, by controlling the different spaces between blocks and changing the length and width of the block, it may be possible to slow down the domino’s spreading. For a larger n , where $n \gg i$, the angle and the angular velocity of the i -th domino exponentially approach θ_m and 0 , respectively, at the same ratio of $k < 1$ as the sequence number i decreases.

3. Domino wave propagation model and Bridge failure

The previous section mainly discussed the methodology and derived the basic theoretical formulas as well as the models that take into account a series of variables. In the third part, this paper applies this model to real-life examples, drawing an analogy between the domino effect and a series of bridge collapses. Specifically, the paper discusses the various ways and probabilities of bridge collapse under different circumstances and attempts to propose effective solutions to mitigate risks. Ch identified eight key factors that cause bridge collapse, as shown in Figure 5.

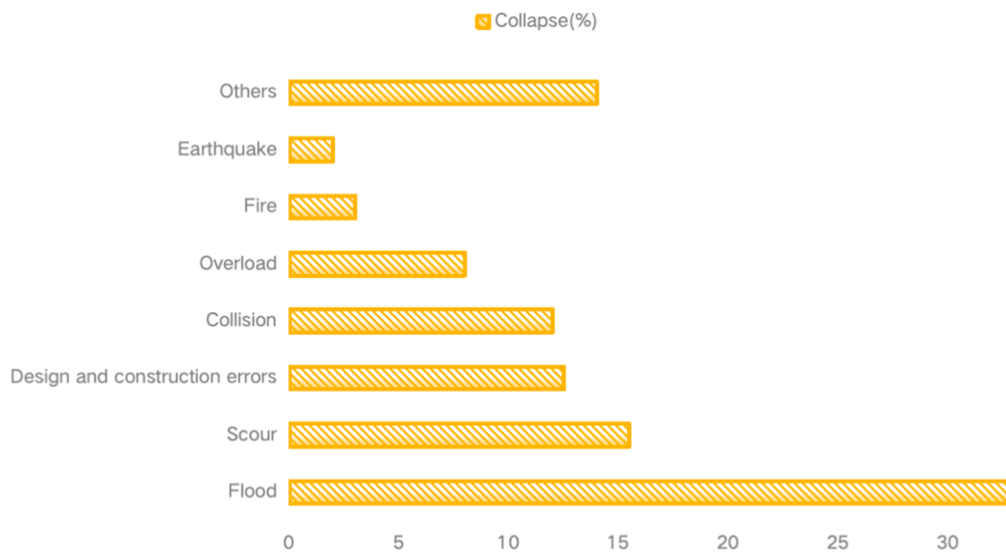


Figure 5: Proportion of collapse causes (Quoted from [International Association for Bridge and Structural Engineering, Bangladesh Group and Doboku Gakkai], Reproduced)

The underestimation only respects the external forces, so the factors of “Others” and “Design and construction errors” will be eliminated.

Earthquake—2 %

Earthquake-induced horizontal and vertical ground motions can lead to shear-bending failures of bridges, expansion-joint failures, shear-key failures, and lateral or longitudinal sliding of beams due to wave phenomena.

Fire—3 %

Collisions of vehicles such as tankers and trucks, multi-vehicle collisions, or construction accidents can cause rapid temperature increases that produce temperature gradients in bridge structures, causing steel joints and concrete to bend because of their different materials and forming the initial stage of the domino-wave spread.

Overload—8 %

The overestimation of bridges' loading capacity will allow overweight trucks, resulting in material fatigue. In this situation, the bridge's service life will be shortened or it will collapse directly.

Collision—12 %

The huge impact force generated by the collision causes serious damage to the bridge structure. Because of the separation of structural components and the centrifugal force of the falling bridge deck, three consecutive spans of the bridge suffer progressive damage.

Scour—15.5 %

Water erosion easily causes deposition of the riverbed; the main factors producing this phenomenon are changes in water velocity or long-term sinking. The foundation of the bridge's load-bearing column will be exposed, lose the horizontal support of the riverbed, and begin to fall in one direction.

Flood—33 %

The definition of flood damage can be found in the paper by Holemba and Matsumoto, which categorizes bridge failure into two main categories: substructure and superstructure. Substructure failure can be further attributed to localized scouring of piers and abutments, contraction and scouring of the riverbed and banks, riverbed siltation, and hydrostatic-load failure. Furthermore, factors such as debris (log) impact, uplift or buoyancy, and overtopping are associated with superstructure failure and are therefore classified as such.

Regardless of the factors of its occurrence, the collected factors are that the collapse of the bridge surface and the abutments, and the remaining standing column cannot support the surface of the bridge. These factors exceed the limit in a part of the bridge or a part of the foundation, and this partial collapse will be the start of the overall collapse, which fits the domino model.

Relatively, scour and flooding in rivers are deeply connected by threatening the riverbed and the upper parts of the bridge column, because their combined proportion is 48.5 % of all six major causes. Scour around bridge piers and abutments is a major cause of flooding. During floods, water velocity increases significantly, leading to flow around piers and abutments. At bridge openings, when water flows through a narrower opening than the upstream channel, it accelerates and exerts greater forces on the bridge columns, leading to contraction scour. The sudden disappearance of the riverbed at the bottom and the impact of turbulent flow at the top can cause uneven forces on the bridge piers.

A uniformly distributed surface-load core can be roughly considered a point-load core. Flow resistance can be divided into shear resistance and resistance due to pressure differences between the upstream and downstream sides of an object, the latter of which creates drag. When a fluid flows past an object, it experiences flow resistance that depends on the shape or form of the object's boundary. The shape of the boundary causes streamline deflection and local acceleration of the fluid. As a result, pressure changes occur from upstream to downstream of the boundary, also known as normal stress. The sum of the forces on the surface creates drag at the boundary and pressure drag on the fluid.

(Seyedkhoei et al.) discuss calculating a bridge-collapse index by estimating the span-to-pier-height ratio. Their paper evaluates the collapse mechanism for three different types of bridges (regular,

semi-regular, and irregular). Furthermore, the pier-height ratio is considered an influencing factor because of the variation in pier heights, R.

$$R = \frac{H}{L} \tag{22}$$

Here, H is the height of the pier; according to the experimental data, the values are 2.8 m, 5.6 m, and 8.4 m. L is the length of the span for all bridges. The ratio R is shown in the table below. The collapse-propagation method in the current study can be classified by the ratio R.

Group number	$R > 0.4$	$R < 0.2$	$0.2 < R < 0.4$
	1	2	3

Figure 6: Different groups of piers based on pier height to span length ratio (Quoted from Seyedkhoei)

They proposed an effect called the pier-height effect. By comparing the impact-force values for short, medium, and tall piers in regular and irregular bridges, they concluded that the likelihood and severity of a crash increase with pier height in both types of bridges. This can be attributed to the higher potential energy of the bridge deck at a greater height.

The span-number effect. By considering both regular and irregular bridges, they concluded that the probability of collapse increases with the number of spans. For example, in a four-span bridge, the deck connection begins to fail at the second peak acceleration recorded during an artificial earthquake. In contrast, in bridges with six or more spans, the deck connection breaks at the first peak acceleration, which is 20 % lower than the second peak acceleration.

4. Conclusion

In Chapter 2, the refinement from the simple model to the relatively complex model traces the path of the domino-wave theory and outlines the progression from the rod model to the block model and then to the three-dimensional model. The modeling process incorporates different variables to address increasingly complex situations. In Chapter 3, the data collected from reports of bridge collapses are first grouped according to the different factors that lead to the bridge-failure sequence; the ways these factors cause collapse are then identified, mainly the breakdown of columns and bridge surfaces, which in turn triggers the domino-wave effect. Overall, the domino-wave phenomenon is the principal cause throughout this process and should receive attention in engineering and architecture. This paper combines the physical domino model with bridge-construction failures in engineering. External forces account for 73.5 % of the cases; floods, fires, earthquakes, overloads, collisions, and scour can all be regarded as external forces. Among these factors, the largest proportion is water flow (flood and scour); this connects to Model 2 in Chapter 2, which achieves a mapping between the theoretical model and the actual situation. In today’s society, bridges, as crucial transportation infrastructure, have safety implications for people’s travel convenience and the protection of lives and property. This paper’s study of domino wave propagation mechanisms and their application to preventing bridge cascading collapse offers a new perspective and approach to bridge engineering. In actual bridge construction and maintenance, considering the impact factors of the domino effect, such as properly designing pier heights, span lengths, and pier spacing, can fundamentally enhance bridges’ anti-collapse capability. Meanwhile, for existing bridges, structural redundancy or damping devices can be added at key nodes according to the theories proposed in this paper. This not only effectively blocks the collapse wave’s transmission path but also extends bridges’ service life to some extent and reduces secondary disasters caused by bridge collapse, bringing significant economic and social benefits. In the future, as relevant research deepens, the domino wave propagation theory is expected to play an important role in preventing the collapse of more types of engineering structures. It will provide strong theoretical support and technical guidance for ensuring the safe and stable operation of various types of infrastructure and promote engineering structural design and safety protection technology to a higher level.

References

- [1] Solanes, J.E.; Gracia, L.; Valls Miro, J. Advances in Human–Machine Interaction, Artificial Intelligence, and Robotics. *Electronics* 2024, 13, 3856.
- [2] Ding, Daniel, et al. “How Fast Are Domino Waves?” ArXiv (Cornell University), Cornell University, Jan. 2022.
- [3] Efthimiou, C. J., and M. D. Johnson. “Domino Waves.” *SIAM Review*, vol. 49, no. 1, Jan. 2007, pp. 111–20.
- [4] FUJII, Fumio. “Modeling the Domino Wave Propagation in Contact Mechanics.” *TRANSACTIONS of the JAPAN SOCIETY of MECHANICAL ENGINEERS Series C*, vol. 78, no. 788, Japan Society Mechanical Engineers, Jan. 2012, pp. 1133–42.
- [5] Holemba, Gibson Ali, and Takashi Matsumoto. “Flood-Induced Bridge Failures in Papua New Guinea.” *MATEC Web of Conferences*, edited by A. Awaludin et al., vol. 258, 2019, p. 03014.
- [6] International Association for Bridge and Structural Engineering. Bangladesh Group, and Doboku Gakkai. *Proceedings of the IABSE-JSCE Joint Conference on Advances in Bridge Engineering-III*, August 21-22, 2015, Dhaka, Bangladesh. Bangladesh Group of Iabse, 2015.
- [7] Lu, G., et al. “Effect of Particle Shape on Domino Wave Propagation: A Perspective from 3D, Anisotropic Discrete Element Simulations.” *Granular Matter*, vol. 16, no. 1, Dec. 2013, pp. 107–14.
- [8] Polaner, David M., and Steven L. Shafer. “Falling dominoes.” *Anesthesia & Analgesia*, vol. 128, no. 4, Apr. 2019, pp. 613–14.
- [9] Seyedkhoei, Amir, et al. “Earthquake-Induced Domino-Type Progressive Collapse in Regular, Semiregular, and Irregular Bridges.” *Shock and Vibration*, vol. 2019, Mar. 2019, pp. 1–18.
- [10] Shi, Tengfei, et al. “Toppling Dynamics of a Mass-Varying Domino System.” *Nonlinear Dynamics*, vol. 98, no. 3, Nov. 2019, pp. 2261–75.